

Preconditioning a hybridizable discontinuous Galerkin method for Navier–Stokes at high Reynolds number

A. D. Lindsay*

S. Rhebergen†

B. S. Southworth‡

December 3, 2025

Abstract

We introduce a preconditioner for a hybridizable discontinuous Galerkin discretization of the linearized Navier–Stokes equations at high Reynolds number. The preconditioner is based on an augmented Lagrangian approach of the full discretization. Unlike standard grad-div type augmentation, however, we consider augmentation based on divergence-conformity. With this augmentation we introduce two different, well-conditioned, and easy to solve matrices to approximate the trace pressure Schur complement. To introduce a completely algebraic solver, we propose to use multifrontal sparse LU solvers using butterfly compression to solve the trace velocity block. Numerical examples demonstrate that the trace pressure Schur complement is highly robust in mesh spacing and Reynolds number and that the multifrontal inexact LU performs well for a wide range of Reynolds numbers.

1 Introduction

In this paper we consider the solution of the stationary incompressible Navier–Stokes equations

$$-\nabla \cdot (2\mu\varepsilon(u)) + \nabla \cdot (u \otimes u) + \nabla p = f \quad \text{in } \Omega, \quad (1a)$$

$$\nabla \cdot u = 0 \quad \text{in } \Omega, \quad (1b)$$

$$u = 0 \quad \text{on } \partial\Omega, \quad (1c)$$

$$\int_{\Omega} p \, dx = 0, \quad (1d)$$

where $\Omega \subset \mathbb{R}^d$ is a polygonal (if $d = 2$) or polyhedral (if $d = 3$) domain, $u : \Omega \rightarrow \mathbb{R}^d$ is the velocity, $p : \Omega \rightarrow \mathbb{R}$ is the (kinematic) pressure, $\varepsilon(u) := (\nabla u + (\nabla u)^T)/2$, $\mu > 0$ is the constant kinematic viscosity, and $f : \Omega \rightarrow \mathbb{R}^d$ is the external body force. We are interested in advection-dominated flows.

To discretize the Navier–Stokes equations, we consider a *hybridizable* discontinuous Galerkin method [12]. Discontinuous Galerkin methods are known to be stable, high-order accurate, and locally conservative methods for advection-dominated flows [13]. Furthermore, if the velocity is $H(\text{div}; \Omega)$ -conforming and exactly divergence-free, then the DG discretization is also energy-stable [14] and pressure-robust [30]. An additional appealing property of hybridizable DG (HDG) methods is that they allow for static condensation, a process in which local degrees-of-freedom are eliminated from the system. Various HDG methods have been introduced for incompressible flows, for example, [9, 15, 20, 33, 35, 37, 45, 47]. We will consider the HDG discretization presented in [48, 49]. This discretization results in an exactly divergence-free and $H(\text{div}; \Omega)$ -conforming

*Computational Frameworks, Idaho National Laboratory, Idaho Falls, ID, 83415, USA (alexander.lindsay@inl.gov), <https://orcid.org/0000-0002-6988-2123>

†Department of Applied Mathematics, University of Waterloo, ON, Canada (srheberg@uwaterloo.ca), <https://orcid.org/0000-0001-6036-0356>

‡Theoretical Division, Los Alamos National Laboratory, Los Alamos, NM 87545, USA (southworth@lanl.gov), <https://orcid.org/0000-0002-0283-4928>

velocity solution using standard DG spaces. The purpose of this paper is to present a new preconditioner for this discretization.

To the best of our knowledge, the only preconditioners shown to be robust in both mesh size and Reynolds number are augmented Lagrangian (AL) type preconditioners (see, for example, [5, 6, 7, 22, 21, 32]). It is for this reason that we consider AL preconditioners in this paper. However, some care must be taken when developing and applying an AL preconditioner to the HDG discretization of [48, 49]. In most AL approaches for Navier–Stokes a consistent penalty term $-\gamma \nabla \nabla \cdot u$ is added to the left hand side of eq. (1a) (either at the algebraic or continuous level). However, in the HDG method of [48, 49] the divergence constraint is a local constraint that is imposed exactly on each cell. A consequence is that this grad-div penalization is local, but more importantly, it vanishes after static condensation. As a result, the Schur complement in the trace pressure remains unchanged and, unfortunately, is still difficult to approximate. For this reason, and further motivated by new linear algebra results on the Schur complement of singularly perturbed saddle point problems we present, we consider a penalty term based on $H(\text{div}; \Omega)$ -conformity, which is amenable to static condensation and also makes for a simple and effective mass-matrix based approximation to the trace pressure Schur complement.

Let us mention that alternative AL approaches for the HDG method for Navier–Stokes have been considered. In [56], during the static condensation step, we only eliminated cell velocity degrees-of-freedom (dofs) instead of cell velocity and cell pressure dofs as we do in the current paper. In this approach the velocity is not exactly divergence-free at intermediate iterations and so a standard grad-div penalty term could be used. However, a large number of iterations were required to reach convergence (see also [53]). An augmented Lagrangian Uzawa iteration method was proposed in [25] for a different HDG method that was introduced in [15, 24]. They show good results with only a small dependence on the Reynolds number for $Re < 1000$ in 2D and, after adding a pseudo-time integration method, also in 3D.

The outline of this paper is as follows. In section 2 we present the HDG discretization for the Navier–Stokes equations. We present new matrix-based theory on preconditioning saddle-point problems with large singular perturbations in section 3, and use this to motivate our proposed AL block preconditioning for the HDG method. Although AL formulations and preconditioning typically allow a simple and effective approximation to the Schur complement, much of the difficulty is transferred to solving the augmented velocity block, which takes the form of an advection-dominated vector advection-diffusion equation with a large symmetric singular perturbation. Here we recognize certain recent developments in the STRUMPACK library [10, 39] are well-suited to solving such problems, and are also algebraic (not requiring the infrastructure of geometric multigrid methods), a particularly useful property in the context of HDG discretizations. We thus combine the STRUMPACK solver for the augmented velocity block with our AL formulation and preconditioning of the coupled system, for a complete method. In section 4 we demonstrate our proposed framework on steady lid-driven cavity and backward-facing step problems up to a Reynolds number of 10^4 . The outer AL-based block preconditioner is demonstrated to be highly robust in mesh spacing and Reynolds number, and the inner STRUMPACK solver performs well, only degrading at very high Reynolds numbers, where the steady state solution becomes very ill-conditioned. However, as discussed in section 4, we expect the algebraic preconditioner proposed here to function effectively for any realistic CFD simulation conditions. We conclude in section 5.

2 HDG for the Navier–Stokes equations

2.1 Notation and finite element spaces

Let $\mathcal{T}_h = \{K\}$ be a simplicial mesh consisting of nonoverlapping cells K and such that $\cup_{K \in \mathcal{T}_h} K = \bar{\Omega}$. Consider two adjacent cells K^+ and K^- . An interior face is defined as $F := \partial K^+ \cap \partial K^-$. A boundary face is defined as a face of cell K that lies on the boundary. We will denote the set of all faces by \mathcal{F}_h and the union of all faces by Γ^0 . The diameter of a cell is denoted by h_K and denote the outward unit normal vector on ∂K by n . Furthermore, for scalar functions u and v , we will write $(u, v)_K = \int_K uv \, dx$, $(u, v)_{\mathcal{T}} = \sum_{K \in \mathcal{T}_h} (u, v)_K$, $\langle u, v \rangle_{\partial K} = \int_{\partial K} uv \, ds$, $\langle u, v \rangle_{\partial \mathcal{T}} = \sum_{K \in \mathcal{T}_h} \langle u, v \rangle_{\partial K}$, $\langle u, v \rangle_F = \int_F uv \, ds$, and $\langle u, v \rangle_{\mathcal{F}} = \sum_{F \in \mathcal{F}_h} \langle u, v \rangle_F$. Similar

notation is used if u, v are vector or matrix functions. We denote the trace of a vector function v from the interior of K^\pm by v^\pm and the outward unit normal to K^\pm by n^\pm . We then define the jump and average operators on an interior face as $[[v \cdot n]] := v^+ \cdot n^+ + v^- \cdot n^-$ and $\{\{v\}\} := \frac{1}{2}(v^+ + v^-)$, respectively. On a boundary face the jump operator is defined as $[[v \cdot n]] := v \cdot n$ while the average operator is $\{\{v\}\} := 0$.

The velocity on Ω and trace of the velocity on Γ^0 are approximated by functions in the following finite element spaces:

$$V_h := \{v_h \in L^2(\Omega)^d : v_h \in P_k(K)^d, \forall K \in \mathcal{T}\}, \quad (2a)$$

$$\bar{V}_h := \{\bar{v}_h \in L^2(\Gamma^0)^d : \bar{v}_h \in P_k(F)^d \forall F \in \mathcal{F}, \bar{v}_h = 0 \text{ on } \partial\Omega\}, \quad (2b)$$

where $P_k(K)$ and $P_k(F)$ are the sets of polynomials of degree at most $k \geq 1$ defined on a cell $K \in \mathcal{T}_h$ and face $F \in \mathcal{F}_h$. Similarly, the pressure on Ω and trace of the pressure on Γ^0 are approximated by functions in

$$Q_h := \{q_h \in L^2(\Omega) : q_h \in P_{k-1}(K), \forall K \in \mathcal{T}\},$$

$$\bar{Q}_h := \{\bar{q}_h \in L^2(\Gamma^0) : \bar{q}_h \in P_k(F) \forall F \in \mathcal{F}\}.$$

Product spaces and pairs in these product spaces will be denoted using boldface. For example, $\mathbf{v}_h := (v_h, \bar{v}_h) \in V_h \times \bar{V}_h =: \mathbf{V}_h$ and $\mathbf{q}_h := (q_h, \bar{q}_h) \in Q_h \times \bar{Q}_h =: \mathbf{Q}_h$.

2.2 The discretization

We consider the following HDG discretization of the Navier–Stokes equations [48]: Find $(\mathbf{u}_h, \mathbf{p}_h) \in \mathbf{V}_h \times \mathbf{Q}_h$ such that for all $(\mathbf{v}_h, \mathbf{q}_h) \in \mathbf{V}_h \times \mathbf{Q}_h$:

$$\mu a_h(\mathbf{u}_h, \mathbf{v}_h) + o_h(u_h; \mathbf{u}_h, \mathbf{v}_h) + b_h(\mathbf{p}_h, v_h) = (f, v)_{\mathcal{T}}, \quad (3a)$$

$$b_h(\mathbf{q}_h, u_h) = 0, \quad (3b)$$

where $a_h(\cdot, \cdot)$ and $o_h(\cdot; \cdot, \cdot)$ are defined as

$$\begin{aligned} a_h(\mathbf{u}, \mathbf{v}) &:= (2\varepsilon(u), \varepsilon(v))_{\mathcal{T}} + \langle 2\alpha h_K^{-1}(u - \bar{u}), v - \bar{v} \rangle_{\partial\mathcal{T}} \\ &\quad - \langle 2\varepsilon(u)n, v - \bar{v} \rangle_{\partial\mathcal{T}} - \langle 2\varepsilon(v)n, u - \bar{u} \rangle_{\partial\mathcal{T}}, \\ o_h(w; \mathbf{u}, \mathbf{v}) &:= - (u \otimes w, \nabla v)_{\mathcal{T}} + \frac{1}{2} \langle (w \cdot n)(u + \bar{u}) + |w \cdot n|(u - \bar{u}), v - \bar{v} \rangle_{\partial\mathcal{T}}, \end{aligned}$$

and where $b_h(\mathbf{q}, v) := b_1(q, v) + b_2(\bar{q}, v)$ in which

$$b_1(q, v) := -(q, \nabla \cdot v)_{\mathcal{T}},$$

$$b_2(\bar{q}, v) := \langle \bar{q}, v \cdot n \rangle_{\partial\mathcal{T}}.$$

The interior penalty parameter $\alpha > 0$ in the definition of $a_h(\cdot, \cdot)$ needs to be chosen sufficiently large for the HDG method to be stable (see [49]). The HDG discretization eq. (3) was shown in [48] to result in a discrete velocity solution $u_h \in V_h$ that is exactly divergence-free on the cells K and globally $H(\text{div}; \Omega)$ -conforming. Consequently, the analysis in [31] shows that this discretization is pressure-robust [30].

2.3 The algebraic formulation

To solve the nonlinear problem eq. (3) we use Picard or Newton iterations. For the sake of presentation we consider a Picard iteration here, but numerical examples in section 4 use Newton iterations.

Let $u \in \mathbb{R}^{n_u}$, $\bar{u} \in \mathbb{R}^{\bar{n}_u}$, $p \in \mathbb{R}_0^{n_p} := \{q \in \mathbb{R}^{n_p} | q \neq 1\}$ and $\bar{p} \in \mathbb{R}^{\bar{n}_p}$ represent the vectors of degrees of freedom for u_h , \bar{u}_h , p_h , and \bar{p}_h , respectively. Furthermore, let $\mathbb{V} := \{\mathbf{v} = [v^T \bar{v}^T]^T : v \in \mathbb{R}^{n_u}, \bar{v} \in \mathbb{R}^{\bar{n}_u}\}$ and $\mathbb{Q} := \{\mathbf{q} = [q^T \bar{q}^T]^T : q \in \mathbb{R}_0^{n_q}, \bar{q} \in \mathbb{R}^{\bar{n}_q}\}$. The forms $a_h(\cdot, \cdot)$, $o_h(w; \cdot, \cdot)$ for w given, $b_1(\cdot, \cdot)$, and $b_2(\cdot, \cdot)$ are

expressed as matrices as follows:

$$\begin{aligned}
a_h(\mathbf{v}_h, \mathbf{v}_h) &= [v^T, \bar{v}^T] \begin{bmatrix} A_{uu} & A_{\bar{u}u}^T \\ A_{\bar{u}u} & A_{\bar{u}\bar{u}} \end{bmatrix} \begin{bmatrix} v \\ \bar{v} \end{bmatrix} \quad \forall \mathbf{v} \in \mathbb{V}, \\
o_h(w; \mathbf{v}_h, \mathbf{v}_h) &= [v^T, \bar{v}^T] \begin{bmatrix} N_{uu} & N_{u\bar{u}} \\ N_{\bar{u}u} & N_{\bar{u}\bar{u}} \end{bmatrix} \begin{bmatrix} v \\ \bar{v} \end{bmatrix} \quad \forall \mathbf{v} \in \mathbb{V}, \\
b_1(q_h, v_h) &= q^T B_{pu} v \quad \forall q \in \mathbb{R}_0^{n_p}, v \in \mathbb{R}^{n_u}, \\
b_2(\bar{q}_h, v_h) &= \bar{q}^T B_{\bar{p}u} v \quad \forall \bar{q}^T \in \mathbb{R}^{\bar{n}_q}, v \in \mathbb{R}^{n_u}.
\end{aligned} \tag{4}$$

Defining also

$$F = \begin{bmatrix} F_{uu} & F_{u\bar{u}} \\ F_{\bar{u}u} & F_{\bar{u}\bar{u}} \end{bmatrix} = \begin{bmatrix} \mu A_{uu} + N_{uu} & \mu A_{\bar{u}u}^T + N_{u\bar{u}} \\ \mu A_{\bar{u}u} + N_{\bar{u}u} & \mu A_{\bar{u}\bar{u}} + N_{\bar{u}\bar{u}} \end{bmatrix}, \tag{5}$$

the algebraic form of the linearized HDG method that needs to be solved at each Picard iteration can be written as:

$$\begin{bmatrix} F_{uu} & B_{pu}^T & F_{u\bar{u}} & B_{\bar{p}u}^T \\ B_{pu} & 0 & 0 & 0 \\ F_{\bar{u}u} & 0 & F_{\bar{u}\bar{u}} & 0 \\ B_{\bar{p}u} & 0 & 0 & 0 \end{bmatrix} \begin{bmatrix} u \\ p \\ \bar{u} \\ \bar{p} \end{bmatrix} = \begin{bmatrix} L_u \\ 0 \\ 0 \\ 0 \end{bmatrix}, \tag{6}$$

where L_u is the vector representation of the right hand side of eq. (3a).

Since the matrices F_{uu} and B_{pu} are block diagonal with one block per cell, u and p can be eliminated locally via static condensation.

3 Preconditioning

In this section we present preconditioning for the linearized HDG method for Navier–Stokes. However, instead of preconditioning eq. (6) directly, we consider a modified version of eq. (6) that is easier to precondition. For this, similar to the Augmented Lagrangian approach of [5], we augment the original problem eq. (6) with a suitable physically consistent penalty term that makes the Schur complement easier to approximate (see section 3.2).

We preface this section by recalling that for solving nonsingular 2×2 block linear systems

$$\begin{bmatrix} A & B \\ C & D \end{bmatrix} \begin{bmatrix} \mathbf{x} \\ \mathbf{y} \end{bmatrix} = \begin{bmatrix} \mathbf{f} \\ \mathbf{g} \end{bmatrix}, \tag{7}$$

a standard approach is to apply a block triangular preconditioner, where one diagonal block is (approximately) inverted and the complementary Schur complement is approximated. For example, a block lower triangular preconditioner would take the form

$$\mathbb{P} = \begin{bmatrix} A & 0 \\ C & \widehat{S} \end{bmatrix}^{-1}, \tag{8}$$

where

$$\widehat{S} \approx S := D - CA^{-1}B. \tag{9}$$

For approximate block triangular or block LDU preconditioners of this form, convergence of fixed-point and minimal residual Krylov methods is fully defined by the convergence of an equivalent method applied to S , preconditioned with \widehat{S} . For more details, see [56]. The important point, which we use as the primary objective in designing our preconditioner, is that the key component to effective preconditioning of eq. (7) is an accurate and computable approximation $\widehat{S}^{-1} \approx S^{-1}$.

In section 3.1 we first present some general results on inverse singular perturbations. We then proceed in section 3.2 to formulate a preconditioner for the HDG method. In this section we will denote the nullspace and range of a matrix A by $\mathcal{N}(A)$ and $\mathcal{R}(A)$, respectively.

3.1 On the inverse of singular perturbations

AL-preconditioning is built around adding a symmetric singular perturbation to the leading block in a 2×2 system, which makes the Schur complement easier to approximate. Here we build on linear algebra theory from [28, Lemma 10], and derive an inverse expansion for the Schur complement of augmented saddle-point systems with respect to perturbation parameter $\gamma \gg 0$.

Lemma 1 (Singular perturbation of saddle-point systems). *Let A be a nonsingular $n \times n$ matrix, $J \neq 0$ be a symmetric, singular $n \times n$ matrix, and B be an $m \times n$ matrix ($m < n$) such that $\mathcal{N}(J) \subseteq \mathcal{N}(B)$ and $\mathcal{R}(B^T) = \mathcal{R}(J)$. Let $\gamma > 0$ be a scalar constant and assume the following matrix is nonsingular:*

$$\mathbb{A} = \begin{bmatrix} A + \gamma J & B^T \\ B & \mathbf{0} \end{bmatrix}.$$

Let P be an orthogonal projection onto $\mathcal{N}(J)$, let $Q = I - P$ denote its complement, and define

$$E_P = P(PAP)^{-1}P, \quad E_Q = Q(QJQ)^{-1}Q,$$

as projected inverses over the range of P and Q . Let $S = -B(A + \gamma J)^{-1}B^T$ denote the Schur complement of \mathbb{A} . The action of S takes the form

$$-S\mathbf{x} = \gamma^{-1}BE_QB^T\mathbf{x} + \gamma^{-2}BR_\gamma B^T\mathbf{x}, \quad (10)$$

where

$$R_\gamma = (I + \gamma^{-1}E_QA(I - E_PA))^{-1}E_QA(I - E_PA)E_Q, \quad (11)$$

and E_PA is a projection onto $\mathcal{N}(J)$.

Proof. A rescaling of the result from [28, Lemma 10] on an inverse expansion for singular perturbations yields the following:¹

$$(A + \gamma J)^{-1}\mathbf{x} = E_P\mathbf{x} + \frac{1}{\gamma}(I - E_PA)E_Q(I - AE_P)\mathbf{x} + \frac{1}{\gamma^2}(I - E_PA)R_\gamma(I - AE_P)\mathbf{x},$$

where

$$R_\gamma = (I + \gamma^{-1}E_Q(A - AE_PA)Q)^{-1}E_QA(I - E_PA)E_Q. \quad (12)$$

Recalling $Q = I - P$,

$$\begin{aligned} (A - AE_PA)Q &= A(I - P(PAP)^{-1}PA)(I - P) \\ &= A(I - P(PAP)^{-1}PA) \\ &= A(I - E_PA), \end{aligned}$$

which yields eq. (11). Then, note that since P projects onto $\mathcal{N}(J) \subseteq \mathcal{N}(B)$, we have $BP = PB^T = \mathbf{0}$. This yields

$$\begin{aligned} -S\mathbf{x} &= B(A + \gamma J)^{-1}B^T\mathbf{x} \\ &= B \left[E_P + \gamma^{-1}(I - E_PA)E_Q(I - AE_P) + \gamma^{-2}(I - E_PA)R_\gamma(I - AE_P) \right] B^T\mathbf{x} \\ &= \gamma^{-1}BE_QB^T\mathbf{x} + \gamma^{-2}BR_\gamma B^T\mathbf{x}, \end{aligned}$$

which is the desired result. □

¹Note, there is a typo in the statement of [28, Lemma 10]; R_ε as occurs in [28, Eq. (34)] should not have a leading factor of ε ; this constant was already accounted for in the inverse expansion in the third term of [28, Eq. (34)].

Lemma 1 provides an inverse expansion for arbitrary symmetric singular perturbation J with nullspace contained within that of B . Often in saddle-point problems and AL-type preconditioners, one chooses J of the specific form $J = B^T M^{-1} B$ for mass matrix M . Such a choice also leads to a further simplification of the action of Schur complement S , which is derived in the following corollary.

Corollary 1 (Augmented Lagrangian Schur complements). *Let A , B , and γ be as in lemma 1, and let M be an $m \times m$ symmetric positive definite (SPD) matrix. Consider the matrix*

$$\mathbb{A} = \begin{bmatrix} A + \gamma B^T M^{-1} B & B^T \\ B & \mathbf{0} \end{bmatrix}. \quad (13)$$

The action of the Schur complement S of \mathbb{A} takes the form

$$-S\mathbf{x} = \gamma^{-1} M\mathbf{x} + \gamma^{-2} B R_\gamma B^T \mathbf{x}.$$

Proof. Let P be the ℓ^2 -orthogonal projection on to the nullspace of $B^T M^{-1} B$, given by

$$P := (I - B^T M^{-1/2} (M^{-1/2} B B^T M^{-1/2})^{-1} M^{-1/2} B) = (I - B^T (B B^T)^{-1} B),$$

and let

$$Q := I - P = B^T M^{-1/2} (M^{-1/2} B B^T M^{-1/2})^{-1} M^{-1/2} B = B^T (B B^T)^{-1} B,$$

denote its complement. Then observe that

$$\begin{aligned} & M^{-1/2} B (Q B^T M^{-1} B Q)^{-1} B^T M^{-1/2} \mathbf{x} \\ &= M^{-1/2} B \left[B^T M^{-1/2} (M^{-1/2} B B^T M^{-1/2})^{-1} M^{-1/2} B B^T M^{-1/2} \right. \\ & \quad \left. M^{-1/2} B B^T M^{-1/2} (M^{-1/2} B B^T M^{-1/2})^{-1} M^{-1/2} B \right]^{-1} B^T M^{-1/2} \mathbf{x} \\ &= M^{-1/2} B (B^T M^{-1/2} M^{-1/2} B)^{-1} B^T M^{-1/2} \mathbf{x}. \end{aligned}$$

To analyze this final term, let $B^T M^{-1/2}$ have SVD $B^T M^{-1/2} = L \Sigma R^T$, for orthogonal left and right singular vectors as columns of $L \in \mathbb{R}^{n \times n}$ and $R \in \mathbb{R}^{m \times m}$, and singular values as nonzero diagonal of $\Sigma \in \mathbb{R}^{n \times m}$. Let $\Sigma^T \Sigma \in \mathbb{R}^{m \times m}$ with positive diagonal entries and $\Sigma \Sigma^T \in \mathbb{R}^{n \times n}$ have m positive diagonal entries and $n - m$ zeros corresponding to the nullspace. Then

$$\begin{aligned} M^{-1/2} B (Q B^T M^{-1} B Q)^{-1} B^T M^{-1/2} \mathbf{x} &= R \Sigma^T L^T (L \Sigma R^T R \Sigma^T L^T)^{-1} L \Sigma R^T \mathbf{x} \\ &= R \Sigma^T (\Sigma \Sigma^T)^{-1} \Sigma R^T \mathbf{x}. \end{aligned}$$

Note we have changed the basis via the SVD, and here the inverse implies we are inverting on the space of nonzero singular values, where $\Sigma \Sigma^T \in \mathbb{R}^{n \times n}$ is nonzero in the leading m diagonal entries and zero in the final $n - m$ entries. In this setting, this is trivially equivalent to a pseudoinverse. The result is that $\Sigma^T (\Sigma \Sigma^T)^{-1} \Sigma = I_m$, implying

$$B (Q B^T M^{-1} B Q)^{-1} B^T M^{-1/2} \mathbf{x} = M^{1/2} \mathbf{x} \iff B (Q B^T M^{-1} B Q)^{-1} B^T \mathbf{y} = M \mathbf{y},$$

for any $\mathbf{x} = M^{1/2} \mathbf{y}$. Given the assumption that M is SPD, this applies for all vectors $\mathbf{y} \in \mathbb{R}^m$. Plugging into eq. (10) completes the proof. \square

Thus to order $1/\gamma$, the Schur complement of eq. (13) can be preconditioned by $\gamma^{-1} M$. It should be noted that this approximation may not be h -independent, in the sense that the residual term R_γ can have a complex eigenvalue/field-of-value structure that may depend on mesh-spacing h . To this end, robust preconditioning may require relatively large γ .

3.2 Preconditioning for HDG

The results of section 3.1 are now used to design preconditioners for the linearized form of the HDG discretization eq. (3) augmented with a suitable penalization term. We begin with a traditional AL-like preconditioning along the lines of $J = BM^{-1}B^T$ (see Corollary 1) in Section 3.2.1. However, such an approach does not facilitate static condensation, so we then use the more general result in Lemma 1 to motivate an approximate preconditioner by focusing on a local representation of the nullspace of B .

3.2.1 AL-like preconditioning

We begin with an augmentation following a traditional AL-approach for incompressible Navier Stokes. Rather than a grad-div augmentation though, define (see, for example, [1])

$$d_h(u, v) = \langle h_F^{-1}[[u \cdot n]], [[v \cdot n]] \rangle_{\mathcal{F}}, \quad (14)$$

and let $D_{uu} \in \mathbb{R}^{n_u \times n_u}$ be the matrix such that $d_h(v_h, v_h) = v^T D_{uu} v$. The following Lemma proves that $d_h(u, v)$ is the weak form associated with an augmentation $D_{uu} = B_{\bar{p}u}^T \bar{M}^{-1} B_{\bar{p}u}$.

Lemma 2. *Let \bar{M} be the trace pressure mass matrix defined by $\|\bar{q}_h\|_p^2 := \bar{q}^T \bar{M} \bar{q}$, where $\|\bar{q}_h\|_p^2 := \sum_{F \in \mathcal{F}_h} h_F \|\bar{q}_h\|_F^2$ for all $\bar{q}_h \in \bar{Q}_h$. It holds that $D_{uu} = B_{\bar{p}u}^T \bar{M}^{-1} B_{\bar{p}u}$.*

Proof. See Appendix A. □

Defining

$$A := \begin{bmatrix} F_{uu} & B_{\bar{p}u}^T & F_{u\bar{u}} \\ B_{\bar{p}u} & 0 & 0 \\ F_{\bar{u}u} & 0 & F_{\bar{u}\bar{u}} \end{bmatrix},$$

as the matrix over $\{u, p, \bar{u}\}$, and $B = \begin{bmatrix} B_{\bar{p}u} & 0 & 0 \end{bmatrix}$, corollary 1 together with lemma 2 suggest the following (block lower-triangular) preconditioner

$$\mathbb{P}_D = \begin{bmatrix} F_{uu} + \gamma D_{uu} & B_{\bar{p}u}^T & F_{u\bar{u}} & 0 \\ B_{\bar{p}u} & 0 & 0 & 0 \\ F_{\bar{u}u} & 0 & F_{\bar{u}\bar{u}} & 0 \\ B_{\bar{p}u} & 0 & 0 & -\gamma^{-1} \bar{M} \end{bmatrix}, \quad (15)$$

as an augmented block preconditioner for the following penalized HDG discretization:

$$\mu a_h(\mathbf{u}_h, \mathbf{v}_h) + o_h(u_h; \mathbf{u}_h, \mathbf{v}_h) + \gamma d_h(u_h, v_h) + b_h(\mathbf{p}_h, v_h) = (f, v_h)_{\mathcal{T}}, \quad (16a)$$

$$b_h(\mathbf{q}_h, u_h) = 0. \quad (16b)$$

In theory, if we eliminate u and p for a reduced system defined only on faces, we arrive at the following condensed preconditioner:

$$\bar{\mathbb{P}}_D = \begin{bmatrix} \bar{F} & 0 \\ -B_{\bar{p}u} \mathcal{P} (F_{uu} + \gamma D_{uu})^{-1} F_{u\bar{u}} & -\gamma^{-1} \bar{M} - B_{\bar{p}u} \mathcal{P} (F_{uu} + \gamma D_{uu})^{-1} B_{\bar{p}u}^T \end{bmatrix}, \quad (17)$$

where

$$\begin{aligned} \bar{F} &= -F_{\bar{u}u} \mathcal{P} (F_{uu} + \gamma D_{uu})^{-1} F_{u\bar{u}} + F_{\bar{u}\bar{u}}, \\ \mathcal{P} &= I - (F_{uu} + \gamma D_{uu})^{-1} B_{\bar{p}u}^T (B_{\bar{p}u} (F_{uu} + \gamma D_{uu})^{-1} B_{\bar{p}u}^T)^{-1} B_{\bar{p}u}. \end{aligned}$$

Above, we proposed a block preconditioner first and then statically condense the 4×4 block system to a 2×2 block system over faces. Alternatively, we can first condense to faces and then define our

preconditioner. Recall the discussion from the beginning of this section regarding convergence of fixed-point and Krylov methods being fully defined by the approximation to the Schur complement. Note that the Schur complement in \bar{p} is identical regardless of whether it is obtained by eliminating the full $\{u, \bar{u}, p\}$ block, or first by condensing to a reduced equation in $\{\bar{u}, \bar{p}\}$ and then forming a Schur complement in \bar{p} . To that end, one can also take corollary 1 and lemma 2 together to imply $-\gamma^{-1}\bar{M}$ is a good approximation to the Schur complement in \bar{p} and apply this to the reduced system, resulting in preconditioner

$$\bar{\mathbb{P}}_{D,M} = \begin{bmatrix} \bar{F} & 0 \\ -B_{\bar{p}u}\mathcal{P}(F_{uu} + \gamma D_{uu})^{-1}F_{u\bar{u}} & -\gamma^{-1}\bar{M} \end{bmatrix}. \quad (18)$$

Note the only difference with $\bar{\mathbb{P}}_D$ in eq. (17) is that here we only include the mass matrix in the approximate Schur complement, whereas in eq. (17) we also include the condensed $\bar{p}\bar{p}$ -block of the system as well.

3.2.2 Preconditioner for static condensation

Unfortunately, it is expensive to apply static condensation to the HDG method eq. (16) because $d_h(\cdot, \cdot)$ couples velocity cell degrees of freedom across multiple cells. As a result, the inverse of $F_{uu} + \gamma D_{uu}$ is typically dense, and we cannot directly construct the reduced system in $\{\bar{u}, \bar{p}\}$. To that end, we seek a local augmentation that maintains the ease of approximating S in \bar{p} , but also facilitates static condensation. We motivate this by considering the more general result on the inverse of singular perturbations, Lemma 1. There we see that the key assumption in choosing an augmentation matrix J is that $\mathcal{N}(J) \subseteq \mathcal{N}(B)$. In Section 3.2.1 we choose $d_h(u, v)$ eq. (14) and the assembled matrix D_{uu} such that $\mathcal{N}(B_{\bar{p}u}) = \mathcal{N}(D_{uu}) = V_h \cap H(\text{div}; \Omega)$ and so also $\mathcal{N}(B) = \mathcal{N}(J)$.

A hybridizable alternative to $d_h(u, v)$, chosen such that the nullspace is a subspace of the nullspace of $d_h(u, v)$, is given by

$$g_h(\mathbf{u}, \mathbf{v}) := \langle h_K^{-1}(u - \bar{u}) \cdot \mathbf{n}, (v - \bar{v}) \cdot \mathbf{n} \rangle_{\partial\mathcal{T}}, \quad (19)$$

which in matrix form is expressed as

$$g_h(\mathbf{v}_h, \mathbf{v}_h) = [v^T, \bar{v}^T]G \begin{bmatrix} v \\ \bar{v} \end{bmatrix} = [v^T, \bar{v}^T] \begin{bmatrix} G_{uu} & G_{uu}^T \\ G_{\bar{u}u} & G_{\bar{u}\bar{u}} \end{bmatrix} \begin{bmatrix} v \\ \bar{v} \end{bmatrix} \quad \forall \mathbf{v} \in \mathbb{V}.$$

Let $R_k(\partial K) := \{\mu \in L^2(\partial K) : \mu|_F \in P_k(F), \forall F \subset \partial K\}$ and let $b_2^K(\bar{q}_h, \mathbf{u}_h) = \langle (u_h - \bar{u}_h) \cdot \mathbf{n}, \bar{q}_h \rangle_{\partial K}$. Then the nullspace of G is given by

$$\mathcal{N}(G) := \{\mathbf{v}_h \in \mathbf{V}_h : b_2^K(\bar{q}_h, \mathbf{u}_h) = 0 \forall \bar{q}_h \in R_k(\partial K), \forall K \in \mathcal{T}_h\}. \quad (20)$$

Note that

$$\begin{aligned} b_2(\bar{q}_h, u_h) &= \sum_{K \in \mathcal{T}_h} \langle u_h \cdot \mathbf{n}, \bar{q}_h \rangle_{\partial K} + \langle u_h \cdot \mathbf{n}, \bar{q}_h \rangle_{\partial\Omega} \\ &= \sum_{K \in \mathcal{T}_h} \langle (u_h - \bar{u}_h) \cdot \mathbf{n}, \bar{q}_h \rangle_{\partial K} = \sum_{K \in \mathcal{T}_h} b_2^K(\bar{q}_h, \mathbf{u}_h), \end{aligned} \quad (21)$$

where the second equality is because $\bar{u}_h \cdot \mathbf{n}$ and \bar{q}_h are single-valued on interior faces and $\bar{u}_h = 0$ on the boundary. This is used to show the following relationship between $\mathcal{N}(G)$ and $\mathcal{N}(D_{uu})$:

$$\begin{aligned} \mathcal{N}(G) &\subset \left\{ \mathbf{v}_h \in \mathbf{V}_h : \sum_{K \in \mathcal{T}_h} b_2^K(\bar{q}_h, v_h) = 0 \forall \bar{q}_h \in \bar{Q}_h \right\} \\ &= \{ \mathbf{v}_h \in \mathbf{V}_h : b_2(\bar{q}_h, v_h) = 0 \forall \bar{q}_h \in \bar{Q}_h \} \\ &= \{ \mathbf{v}_h \in \mathbf{V}_h : v_h \in V_h \cap H(\text{div}, \Omega) \} \\ &= [V_h \cap H(\text{div}, \Omega)] \times \bar{V}_h \\ &= \mathcal{N}(D_{uu}) \times \bar{V}_h. \end{aligned} \quad (22)$$

In other words, the nullspace of G is smaller than that of D_{uu} as $\mathbf{v}_h \in \mathcal{N}(G)$ requires $\mathbf{v}_h \cdot \mathbf{n} = \bar{\mathbf{v}}_h \cdot \mathbf{n}$ on all faces in addition to $\mathbf{v}_h \in V_h \cap H(\text{div}; \Omega)$.

By nature of $\mathcal{N}(G) \subset \mathcal{N}(D_{uu})$, Lemma 1 still naturally applies. In Corollary 1 and section 3.2.1 we are able to express the leading order term in \mathcal{S} specifically as a mass matrix. Here we no longer have the analytical representation of the leading term in γ , but posit that the mass matrix remains a good approximation to the leading order term in γ , $BE_Q B^T$, a hypothesis confirmed in experiments in section 4. Replacing the augmentation D_{uu} in eq. (15) with the matrix form of $g_h(\cdot, \cdot)$, we find the following block preconditioner

$$\mathbb{P}_G = \begin{bmatrix} F_{uu} + \gamma G_{uu} & B_{pu}^T & F_{u\bar{u}} + \gamma G_{u\bar{u}}^T & 0 \\ B_{pu} & 0 & 0 & 0 \\ F_{\bar{u}u} + \gamma G_{\bar{u}u} & 0 & F_{\bar{u}\bar{u}} + \gamma G_{\bar{u}\bar{u}} & 0 \\ B_{\bar{p}u} & 0 & 0 & -\gamma^{-1} \bar{M} \end{bmatrix}, \quad (23)$$

as an augmented block preconditioner for the following penalized HDG discretization:

$$\mu a_h(\mathbf{u}_h, \mathbf{v}_h) + o_h(u_h; \mathbf{u}_h, \mathbf{v}_h) + \gamma g_h(\mathbf{u}_h, \mathbf{v}_h) + b_h(\mathbf{p}_h, v_h) = (f, v)_T, \quad (24a)$$

$$b_h(\mathbf{q}_h, u_h) = 0. \quad (24b)$$

Since F_{uu} , B_{pu} , and G_{uu} are block diagonal with one block per cell, we can directly eliminate u and p from eq. (24) for a reduced system defined only on faces. The corresponding condensed preconditioner is given by

$$\bar{\mathbb{P}}_G = \begin{bmatrix} \bar{F}^g & 0 \\ -B_{\bar{p}u} \mathcal{P}^g (F_{uu} + \gamma G_{uu})^{-1} F_{u\bar{u}}^g & -\gamma^{-1} \bar{M} - B_{\bar{p}u} \mathcal{P}^g (F_{uu} + \gamma G_{uu})^{-1} B_{\bar{p}u}^T \end{bmatrix}, \quad (25)$$

where

$$\begin{aligned} \bar{F}^g &= -F_{\bar{u}u}^g \mathcal{P}^g (F_{uu} + \gamma G_{uu})^{-1} F_{u\bar{u}}^g + F_{\bar{u}\bar{u}}^g, \\ \mathcal{P}^g &= I - (F_{uu} + \gamma G_{uu})^{-1} B_{pu}^T (B_{pu} (F_{uu} + \gamma G_{uu})^{-1} B_{pu}^T)^{-1} B_{pu}, \end{aligned}$$

and $F_{uu}^g = F_{\bar{u}u} + \gamma G_{\bar{u}u}$, $F_{u\bar{u}}^g = F_{u\bar{u}} + \gamma G_{u\bar{u}}^T$, $F_{\bar{u}\bar{u}}^g = F_{\bar{u}\bar{u}} + \gamma G_{\bar{u}\bar{u}}$.

As discussed in Section 3.2.1, the Schur complement in \bar{p} is identical before and after static condensation. Thus one could also first statically condense the augmented system, and then note that the Schur complement in \bar{p} is well approximated by a mass-matrix, resulting in the similar preconditioner

$$\bar{\mathbb{P}}_{G,M} = \begin{bmatrix} \bar{F}^g & 0 \\ -B_{\bar{p}u} \mathcal{P}^g (F_{uu} + \gamma G_{uu})^{-1} F_{u\bar{u}}^g & -\gamma^{-1} \bar{M} \end{bmatrix}. \quad (26)$$

Remark 1. While the solution $(\mathbf{u}_h, \mathbf{p}_h) \in \mathbf{V}_h \times \mathbf{Q}_h$ to eq. (3) and eq. (16) are the same, the solution to eq. (3) and eq. (24) are not due to eq. (22). However, g_h is a consistent penalization term that does not affect the well-posedness and accuracy of the discretization; see Appendix B.

3.3 Solving the augmented velocity block

The preconditioners $\bar{\mathbb{P}}_G$ in eq. (25) and $\bar{\mathbb{P}}_{G,M}$ in eq. (26) still require the (action of the) inverse of \bar{F}^g and either $-\gamma^{-1} \bar{M} - B_{\bar{p}u} \mathcal{P}^g (F_{uu} + \gamma G_{uu})^{-1} B_{\bar{p}u}^T$ or $-\gamma^{-1} \bar{M}$. The two trace pressure Schur complement terms are relatively well-conditioned and easy to solve. Conversely, by creating simple (and effective) approximate Schur complements, we have transferred much of this difficulty to solving the augmented velocity block.

Before static condensation, the augmented velocity block corresponds to an advection dominated advection-diffusion equation with a large symmetric singular perturbation. Each of these classes of problems, advection-dominated problems and singular perturbations, are independently quite challenging to solve in a fast and scalable way. When applicable, multilevel methods are typically the most efficient linear solvers for large

Table 1: Representative iteration counts for application of the preconditioner proposed in [4] to the velocity block of a Q2-Q1 Taylor–Hood discretization of a lid-driven cavity. Here we use a block lower triangular preconditioner with “exact” Schur complement up to numerical precision (see Appendix C for details on PETSc KSP Schur complement preconditioning). Each KSP preconditioner application requires two velocity block solves, one that is directly part of the lower triangular KSP preconditioner (A in (8)), and one inner solve required to compute the action of the Schur complement (see S in (9)) when computing a residual in the KSP. For each simulation case, two numbers are reported unless GMRES did not converge (DNC). The first is the number of iterations required for the velocity block solve in the lower triangular KSP preconditioner. The second is the number of iterations required for the inner KSP velocity block solves to compute the action of the Schur complement. The linear solver relative tolerance is 10^{-2} for each KSP with restart after 300 Krylov basis vectors. When applied to the inner KSP velocity solves, the preconditioner performs exceptionally well, but when applied to the lower KSP velocity solves, the preconditioner performs poorly except for very small problems. Moreover, the velocity block solves in the lower triangular KSP are arguably the most important, as these are fundamental to any block preconditioner, even when using an inexact Schur complement as in (8) and used in numerical results in section 4.

Cells	DOFs	Re = 10	Re = 10^2	Re = $5 \cdot 10^2$
16	187	16,2	18,2	24,2
64	659	58,2	DNC,2	DNC,2
256	2467	177,2	DNC,2	DNC,2

sparse systems, particularly arising from differential operators. Geometric multigrid (GMG) methods applied to advection-dominated problems almost always require semi-coarsening and/or line/plane relaxation to capture the advection on coarse grids. Such techniques require structured grids and provide poor parallel scaling, as the line/plane relaxation typically spans many processes. The only exception we are aware of is the patch-relaxation multigrid methods in [22, 21] that prove robust for certain discretizations of high-Reynolds number incompressible flow problems, using a local patch-based relaxation rather than full line/plane relaxation. Why these methods are effective on high-Reynolds number incompressible problems remains an open question. However, it should be pointed out that to the best of our knowledge the preconditioner and patch-based GMG in [22, 21] are the only fast solvers in the literature that have demonstrated robust performance in mesh spacing and Reynolds number, and are naturally parallelizable.

The extension of GMG methods to HDG discretizations is nontrivial [11, 25, 40, 44]. We are also interested in algebraic approaches for practical reasons, where large-scale codes, particularly of the multi-physics type, do not always maintain a full mesh hierarchy as needed for GMG. Recent work has developed fast AIR-algebraic MG (AMG) methods for certain advection-dominated problems [42, 41], including HDG advection-diffusion systems [54]. However, these methods rely heavily on the matrix structure arising from an advection-dominated problem, and a large symmetric singular perturbation ruins this structure and the corresponding convergence of AIR-AMG. A recent paper on preconditioning singular perturbations $A + \gamma UU^T$ [4] offered one route to combine AIR-AMG with solvers directly for the singular perturbation, e.g. [18, 36]. However, we have not found the method proposed in [4] to be robust for our problems. Specifically, the performance of the preconditioner proposed in [4] appears to be highly sensitive to the linear system right-hand side as illustrated in table 1.

Post static condensation, the equation is arguably more complicated because the two distinct components are intertwined in complex ways. This makes it challenging to take advantage of certain known structure such as the symmetric singular perturbation with known kernel. Other algebraic preconditioners often used in a black-box manner are approximate sparse inverse methods, such as incomplete LU (ILU). Unfortunately, our experience has been that ILU is typically not effective on advection-dominated problems. For example, on the 2D lid-driven cavity problem we consider in Section 4, ILU(10) converges well for a Reynolds number of 1, but at a Reynolds number of 10, GMRES with no restart preconditioned by ILU(10) does not converge in 300 iterations, and performance further degrades with increasing Reynolds number.

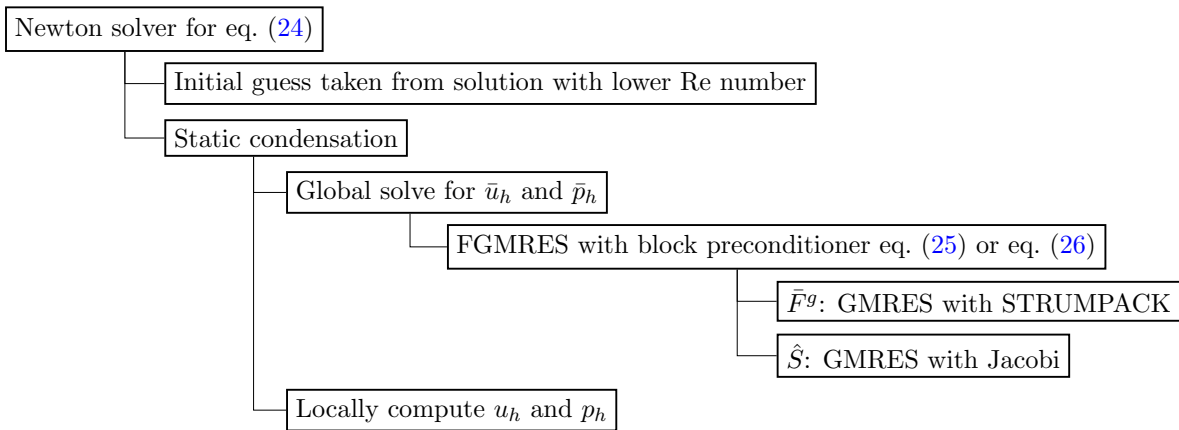


Figure 1: Solver diagram.

Recently, a new class of methods based on multifrontal sparse LU solvers using butterfly compression have been developed in the STRUMPACK library, targeting wave equations and sparse systems where the frontal matrices are effectively high rank and not amenable to the low rank approximations used for elliptic problems [10, 39]. These methods are in principle direct solvers, with inner approximations and memory compression techniques to accelerate performance and reduce memory requirements. Between needing an algebraic solver that is effectively black box and solving low regularity problems with high Reynolds numbers, the methods developed in [10, 39] are well-suited to the challenges arising in augmented high Reynolds number flow. Thus, to solve the statically condensed velocity field from the augmented system, \bar{F}^g , we use GMRES with multifrontal inexact LU by STRUMPACK. As demonstrated in Section 4, the performance is quite good and able to solve challenging high Reynolds number problems efficiently.

4 Numerical examples

We use Newton’s method with continuation to solve eq. (24). At each Newton step the linear problems are statically condensed and the global problems are solved using FGMRES preconditioned with block preconditioners $\bar{\mathbb{P}}_G$ in eq. (25) or $\bar{\mathbb{P}}_{G,M}$ in eq. (26), based on the block lower triangular preconditioner in (8) with approximate Schur complement.’ The condensed velocity block in the preconditioner is solved using GMRES preconditioned with STRUMPACK. The Schur complement is solved using FGMRES with diagonal Jacobi preconditioning. See fig. 1 for the solver diagram. The numerical examples are implemented in MOOSE [27] with solver support from PETSc [2, 3] and STRUMPACK [39, 10].

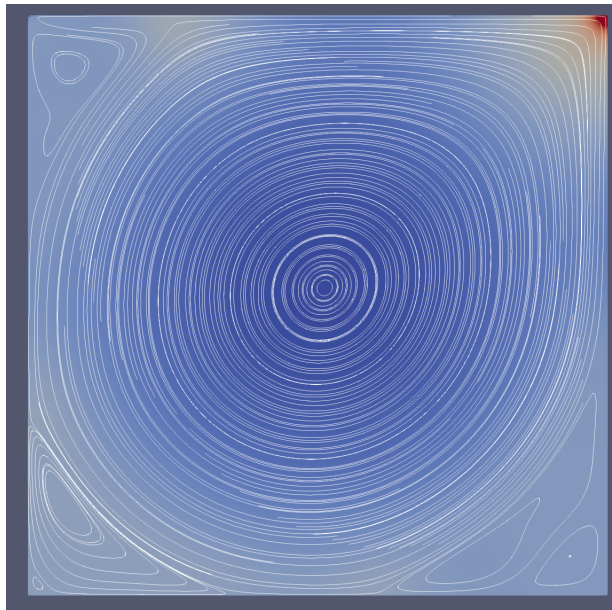
All simulations use the penalty parameter $\alpha = 10k^2$, with k the degree of the polynomial approximation, and preconditioning parameter $\gamma = 10^4$. For the numerical examples we will refer to the Reynolds number which is defined as $\text{Re} := UL/\mu$ with U the characteristic velocity and L the characteristic length scale of the flow.

4.1 Test cases

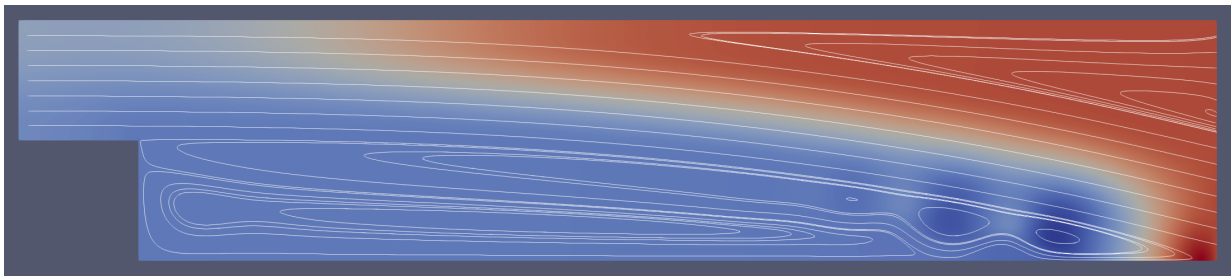
We consider the lid-driven cavity and backward-facing step problems. For the lid-driven cavity problem we set $\Omega = (0, 1)^2$, impose $u = (1, 0)$ on the boundary $x_2 = 1$ and set $u = 0$ on the remaining boundaries. For the backward-facing step we consider $\Omega = ([0, 10] \times [0, 2]) \setminus ([0, 1] \times [0, 1])$ and impose $u = (4(2 - x_2)(x_2 - 1), 0)$ on the boundary $x_1 = 0$, outflow boundary at $x_1 = 10$, and $u = 0$ elsewhere. For both test cases, the characteristic velocity and characteristic length are unity so that $\text{Re} = 1/\mu$. The meshes for the lid-driven cavity problem are regular triangular meshes while the meshes for the backward-facing step problem have been taken from [23].

For both test cases we follow [21] and consider continuation in the Reynolds number, using the previous lower Reynolds number as initial guess for Newton’s method for the current Reynolds number. For the

lid-driven cavity problem we solve for $Re = 1$, $Re = 10$, $Re = 100$ and then in steps of 250 until $Re = 10\,000$. For the backward-facing step we solve for $Re = 1$, $Re = 10$, $Re = 50$, $Re = 100$, $Re = 150$, $Re = 200$, $Re = 250$, $Re = 300$, $Re = 350$, $Re = 400$ and then in steps of 200 until $Re = 10\,000$. The initial guess for $Re = 1$ is the zero vector. The absolute and relative tolerances for the nonlinear solver are 10^{-7} and 10^{-8} respectively. The outer linear solver relative tolerance is 10^{-4} while the inner linear solver relative tolerances for the condensed velocity block and condensed Schur complement are both 10^{-2} . The outer and inner linear solver absolute tolerances are 10^{-9} and 10^{-8} respectively. Convergence for both outer and inner linear solvers is determined based on the unpreconditioned residual norm. Plots of the solutions at $Re = 10\,000$ for the lid-driven cavity and backward-facing step are given in fig. 2.



(a) Lid-driven cavity.



(b) Backward-facing step.

Figure 2: Pressure colormaps plus streamline plots of the lid-driven cavity and backward-facing step problems with $Re = 10\,000$

4.2 Results

In table 2 and table 3 we present the number of iterations needed to converge for various Reynolds numbers when $k = 2$ and when using the HDG discretization with eq. (25) and eq. (26) respectively. We report three numbers which describe the solve (see fig. 1). The first is the number of Newton iterations. The second is the maximum number of outer FGMRES iterations observed over the Newton solve which is an implicit measure of the quality of the Schur complement approximation. The final number is the maximum number of GMRES iterations to solve \bar{F}^g . We also present the average Newton solve time, averaged over all Reynolds numbers, divided by the number of degrees of freedom per process. We observe that the Schur complement approximation, as measured by the second iteration count, is robust with respect to both number of degrees

Table 2: Solver results for two dimensional test cases with HDG discretization using the preconditioner eq. (25). The first column is the number of processes.

p	Cells	Total dofs	Condensed dofs	Re = 1	10	10 ²	10 ³	10 ⁴	time/100k local dofs
Lid-driven cavity problem									
1	2048	58 944	28 224	2,10,1	2,14,1	3,10,1	3,10,1	2,10,1	17.3
4	8192	234 624	111 744	2,10,1	2,14,1	3,10,1	3,11,1	2,10,1	18.2
16	32 768	936 192	444 672	2,10,2	2,13,1	3,10,11	3,10,11	1,10,7	28.9
Backward-facing step problem									
1	3203	92 199	44 154	2,10,1	2,11,1	3,11,1	3,11,1	2,11,1	21.5
4	12 812	366 969	174 789	2,10,1	2,11,1	3,11,1	3,11,1	2,11,1	19.5
16	51 284	1 464 222	695 502	2,10,1	2,11,1	3,12,1	3,12,1	2,11,1	28.0

Table 3: Solver results for two dimensional test cases with HDG discretization using the preconditioner eq. (26). The first column is the number of processes.

p	Cells	Total dofs	Condensed dofs	Re = 1	10	10 ²	10 ³	10 ⁴	time/100k local dofs
Lid-driven cavity problem									
1	2048	58 944	28 224	2,6,1	2,6,1	3,6,1	3,6,1	2,6,1	13.2
4	8192	234 624	111 744	2,6,1	2,6,1	3,5,1	3,6,1	2,5,1	17.4
16	32 768	936 192	444 672	2,6,2	2,7,3	3,7,11	3,8,11	1,7,9	27.3
Backward-facing step problem									
1	3203	92 199	44 154	2,9,1	2,10,1	3,10,1	3,10,1	2,10,1	21.3
4	12 812	366 969	174 789	2,9,1	2,10,1	3,10,1	3,10,1	2,10,1	19.2
16	51 248	1 464 222	695 502	2,9,1	2,11,1	3,11,1	3,10,1	2,10,1	27.4

of freedom and Reynolds number. This FGMRES iteration count is significantly lower for the lid driven case and slightly lower for the backwards facing step case when using eq. (26) compared to eq. (25). We observe that the multifrontal inexact LU used to solve \bar{F}^g , as measured by iteration counts, is robust with respect to both number of degrees of freedom and the Reynolds number up to a critical case-dependent problem size. We do not reach that size for the backward facing step cases considered for the paper, but we do for the lid driven problem. For the lid driven case with 32 768 cells we observe the number of iterations required to approximately solve \bar{F}^g increase substantially (5x) when moving from diffusion to advection dominated regimes. This notably affects the weak scaling of the solver with the average solve time increasing by 60% between 8192 cell and 32 768 cell cases whereas the average solve time only increased by 5% when using eq. (25) and 30% when using eq. (26) at the previous refinement level. When performing the first refinement for the backwards facing step we observe the desired weak scaling: constant average solve time (actually a 10% decrease). However, at the next refinement level we note a $\sim 40\%$ increase in average solve time even with a constant number of iterations required to approximately solve \bar{F}^g . We attribute this to the non-linear complexity of LU factorization.

The preconditioners in this manuscript are introduced for the HDG discretization of the Navier–Stokes equations. However, they can also be applied to an embedded-hybridizable discontinuous Galerkin (EDG-HDG) [51] discretization in which \bar{V}_h in eq. (2b) is replaced by $\bar{V}_h \cap C^0(\Gamma^0)$. In table 4 we present results using the EDG-HDG discretization combined with the preconditioner eq. (26). The results are qualitatively similar to those for HDG. For the lid driven cavity case we note that the number of strumpack iterations required to solve \bar{F}^g for the most refined case is lower due to the reduced number of degrees of freedom present in the EDG-HDG system and consequently lower compression loss. We note a 100% increase in the average solve time when moving to the most refined backwards facing step case. We attribute this to the increase in number of iterations required to solve \bar{F}^g as well as the non-linear complexity of LU factorization.

Table 4: Solver results for two dimensional test cases with EDG-HDG discretization using the preconditioner eq. (26). The first column is the number of processes.

p	Cells	Total dofs	Condensed dofs	Re = 1	10	10 ²	10 ³	10 ⁴	time/100k local dofs
Lid-driven cavity problem									
1	2048	48 578	17 858	2,6,1	2,6,1	3,6,1	3,6,1	2,6,1	16.7
4	8192	193 410	70 530	2,6,1	2,5,1	3,4,1	3,6,1	2,5,1	14.3
16	32 768	771 842	280 322	2,6,1	2,5,1	3,5,2	3,7,2	1,7,3	18.2
Backward-facing step problem									
1	12 812	302 505	110 325	2,9,1	2,10,1	3,10,1	3,10,1	2,10,1	12.6
4	51 284	1 207 172	438 452	2,9,1	2,10,1	3,11,1	3,10,1	2,10,1	15.6
16	204 992	4 822 998	1 748 118	2,8,2	2,10,3	3,11,5	2,11,10	2,10,18	30.5

4.3 Further discussion

As stated above, the preconditioners developed in this work are robust until reaching a critical threshold of problem size and Reynolds number. We believe this is an important observation; running the backwards facing step with a Reynolds number of 6×10^5 using a $k - \epsilon$ turbulence model yields an effective Reynolds number (when including the effect of the turbulent viscosity) of 9×10^2 [43, 38]. Moreover, wall functions in Reynolds-Averaged Navier–Stokes (RANS) models like $k - \epsilon$ generally constrain the minimum element size near boundaries such that the overall problem size is not large [34, 57, 46]; we observe strong performance for a large range of Reynolds numbers for moderate problem sizes. Large Eddy Simulation (LES) models [55, 16, 52], another possible target area for HDG, have much higher effective Reynolds numbers than RANS, but in this case simulations are transient with sufficiently small timesteps such that explicit time integration can be used or such that the implicit system is significantly easier to solve due to increasing diagonal dominance. In summary we expect the algebraic preconditioner proposed here to function effectively for realistic CFD simulation conditions.

5 Conclusions

We introduce an AL-like block preconditioner for a hybridizable discontinuous Galerkin discretization of the linearized Navier–Stokes equations at high Reynolds number. New linear algebra theory related to AL preconditioning is used to motivate the new preconditioners, and sparse direct solvers from STRUMPACK are used to solve the inner blocks of the block coupled system. The nonlinearities are resolved using Newton iterations with continuation in Reynolds number, and results are demonstrated on the lid-driven cavity and backward facing step problems. The block preconditioner is shown to be highly robust and effective, and STRUMPACK solvers are demonstrated to be moderately robust, most importantly on realistic Reynolds numbers that would arise in CFD simulations with implicit time stepping or where steady state solutions make sense.

Acknowledgments

BSS was supported by the DOE Office of Advanced Scientific Computing Research Applied Mathematics program through Contract No. 89233218CNA000001. Los Alamos National Laboratory Report LA-UR-25-31645. SR was supported by the Natural Sciences and Engineering Research Council of Canada through the Discovery Grant program (RGPIN-2023-03237). ADL was supported by Lab Directed Research and Development program funding at Idaho National Laboratory under contract DE-AC07-05ID14517.

The authors thank Abdullah Ali Sivas for discussions on solvers for HDG methods. The authors also thank Pierre Jolivet for extensive discussion and experimentation on preconditioning for the augmented and condensed velocity block.

References

- [1] M. Akbas, A. Linke, L. G. Rebholz, and P. W. Schroeder. The analogue of grad-div stabilization in DG methods for incompressible flows: Limiting behavior and extension to tensor-product meshes. *Comput. Methods Appl. Mech. Engrg.*, 341:917–938, 2018.
- [2] S. Balay, S. Abhyankar, M. F. Adams, S. Benson, J. Brown, P. Brune, K. Buschelman, E. Constantinescu, L. Dalcin, A. Dener, V. Eijkhout, J. Faibussowitsch, W. D. Gropp, V. Hapla, T. Isaac, P. Jolivet, D. Karpeev, D. Kaushik, M. G. Knepley, F. Kong, S. Kruger, D. A. May, L. Curfman McInnes, R. Tran Mills, L. Mitchell, T. Munson, J. E. Roman, K. Rupp, P. Sanan, J. Sarich, B. F. Smith, S. Zampini, H. Zhang, H. Zhang, and J. Zhang. PETSc/TAO users manual. Technical Report ANL-21/39 - Revision 3.19, Argonne National Laboratory, 2023.
- [3] S. Balay, W. D. Gropp, L. Curfman McInnes, and B. F. Smith. Efficient management of parallelism in object oriented numerical software libraries. In E. Arge, A. M. Bruaset, and H. P. Langtangen, editors, *Modern Software Tools in Scientific Computing*, pages 163–202. Birkhäuser Press, 1997.
- [4] M. Benzi and C. Faccio. Solving linear systems of the form by preconditioned iterative methods. *SIAM Journal on Scientific Computing*, 46(2):S51–S70, 2024.
- [5] M. Benzi and M. A. Olshanskii. An augmented Lagrangian-based approach to the Oseen problem. *SIAM J. Sci. Comput.*, 28(6):2095–2113, 2006.
- [6] M. Benzi and M. A. Olshanskii. Field-of-values convergence analysis of augmented Lagrangian preconditioners for the linearized Navier–Stokes problem. *SIAM J. Numer. Anal.*, 49(2):770–788, 2011.
- [7] M. Benzi, M. A. Olshanskii, and Z. Wang. Modified augmented Lagrangian preconditioners for the incompressible Navier–Stokes equations. *Int. J. Numer. Mesh. Fluids*, 66:486–508, 2011.
- [8] F. Brezzi and M. Fortin. *Mixed and Hybrid Finite Element Methods*, volume 15 of *Springer Series in Computational Mathematics*. Springer–Verlag New York Inc., 1991.
- [9] A. Cesmelioglu, B. Cockburn, and W. Qiu. Analysis of a hybridizable discontinuous Galerkin method for the steady-state incompressible Navier–Stokes equations. *Math. Comp.*, 86:1643–1670, 2017.
- [10] L. Claus, P. Ghysels, Y. Liu, T. A. Nhan, R. Thirumalaisamy, A. P. S. Bhalla, and S. Li. Sparse approximate multifrontal factorization with composite compression methods. *ACM Transactions on Mathematical Software*, 49(3):1–28, 2023.
- [11] B. Cockburn, O. Dubois, J. Gopalakrishnan, and S. Tan. Multigrid for an HDG method. *IMA J. Numer. Anal.*, 34(4):1386–1425, 2014.
- [12] B. Cockburn, J. Gopalakrishnan, and R. Lazarov. Unified hybridization of discontinuous Galerkin, mixed, and continuous Galerkin methods for second order elliptic problems. *SIAM J. Numer. Anal.*, 47(2):1319–1365, 2009.
- [13] B. Cockburn, G. Kanschat, and D. Schötzau. The local discontinuous Galerkin method for linearized incompressible fluid flow: a review. *Computers & Fluids*, 34:491–506, 2005.
- [14] B. Cockburn, G. Kanschat, and D. Schötzau. A note on discontinuous Galerkin divergence-free solutions of the Navier–Stokes equations. *Journal of Scientific Computing*, 31:61–73, 2007.
- [15] B. Cockburn and F. J. Sayas. Divergence-conforming HDG methods for Stokes flows. *Math. Comp.*, 83:1571–1598, 2014.
- [16] James W Deardorff. A numerical study of three-dimensional turbulent channel flow at large reynolds numbers. *Journal of Fluid Mechanics*, 41(2):453–480, 1970.

- [17] D. A. Di Pietro and A. Ern. *Mathematical Aspects of Discontinuous Galerkin Methods*, volume 69 of *Mathématiques et Applications*. Springer–Verlag Berlin Heidelberg, 2012.
- [18] V. Dobrev, T. Kolev, C. S. Lee, V. Tomov, and P. S. Vassilevski. Algebraic hybridization and static condensation with application to scalable $H(\text{div})$ preconditioning. *SIAM J. Sci. Comput.*, 41(3):B425–B447, 2019.
- [19] S. Du and F.-J. Sayas. *An invitation to the theory of the hybridizable discontinuous Galerkin method. Projections, Estimates, Tools*. Springer Briefs in Mathematics. Springer, 2019.
- [20] H. Egger and C. Waluga. hp analysis of a hybrid DG method for Stokes flow. *IMA J. Numer. Anal.*, 33:687–721, 2013.
- [21] P. E. Farrell, L. Mitchell, L. R. Scott, and F. Wechsung. A Reynolds-robust preconditioner for the Scott–Vogelius discretization of the stationary incompressible Navier–Stokes equations. *SMAI J. Comput. Math.*, 7:75–96, 2021.
- [22] P. E. Farrell, L. Mitchell, and F. Wechsung. An Augmented Lagrangian preconditioner for the 3D stationary incompressible Navier–Stokes equations at high Reynolds number. *SIAM J. Sci. Comput.*, 41(5):A3073–3096, 2019.
- [23] firedrake zenodo. Software used in 'An augmented Lagrangian preconditioner for the 3D stationary incompressible Navier–Stokes equations at high Reynolds number', June 2019.
- [24] G. Fu, Y. Jin, and W. Qiu. Parameter-free superconvergent $H(\text{div})$ -conforming HDG methods for the Brinkman equations. *IMA J. Num. Anal.*, 39(2):957–982, 2019.
- [25] G. Fu and W. Kuang. hp -Multigrid for a divergence-conforming HDG scheme for the incompressible flow problems. *Journal of Scientific Computing*, 100:16, 2024.
- [26] P. Hansbo and M. G. Larson. Discontinuous Galerkin methods for incompressible and nearly incompressible elasticity by Nitsche’s method. *Comput. Methods Appl. Mech. Engrg.*, 191:1895–1908, 2002.
- [27] Logan Harbour, Guillaume Giudicelli, Alexander D Lindsay, Peter German, Joshua Hansel, Casey Icenhour, Mengnan Li, Jason M Miller, Roy H Stogner, Patrick Behne, et al. 4.0 moose: Enabling massively parallel multiphysics simulation. *SoftwareX*, 31:102264, 2025.
- [28] T. S. Haut, B. S. Southworth, P. G. Maginot, and V. Z. Tomov. Diffusion synthetic acceleration preconditioning for discontinuous Galerkin discretizations of s_n transport on high-order curved meshes. *SIAM Journal on Scientific Computing*, 42(5):B1271–B1301, 2020.
- [29] J. S. Howell and N. J. Walkington. Inf-sup conditions for twofold saddle point problems. *Numer. Math.*, 118:663–693, 2011.
- [30] V. John, A. Linke, C. Merdon, M. Neilan, and L. G. Rebholz. On the divergence constraint in mixed finite element methods for incompressible flows. *SIAM Rev.*, 59(3):492–544, 2017.
- [31] K. L. A. Kirk and S. Rhebergen. Analysis of a pressure-robust hybridized discontinuous Galerkin method for the stationary Navier–Stokes equations. *J. Sci. Comput.*, 81(2):881–897, 2019.
- [32] F. Laakmann, P. E. Farrell, and L. Mitchell. An augmented Lagrangian preconditioner for the magnetohydrodynamics equations at high Reynolds and coupling numbers. *SIAM Journal on Scientific Computing*, 44(4):B1018–B1044, 2022.
- [33] R. J. Labeur and G. N. Wells. Energy stable and momentum conserving hybrid finite element method for the incompressible Navier–Stokes equations. *SIAM J. Sci. Comput.*, 34(2):A889–A913, 2012.

- [34] Brian Edward Launder and Dudley Brian Spalding. The numerical computation of turbulent flows. In *Numerical prediction of flow, heat transfer, turbulence and combustion*, pages 96–116. Elsevier, 1983.
- [35] P. L. Lederer, C. Lehrenfeld, and J. Schöberl. Hybrid discontinuous Galerkin methods with relaxed $H(\text{div})$ -conformity for incompressible flows. Part I. *SIAM J. Numer. Anal.*, 56(4):2070–2094, 2018.
- [36] C. H. Lee and P. S. Vassilevski. Parallel solver for $H(\text{div})$ problems using hybridization and AMG. In *Domain Decomposition Methods in Science and Engineering XXIII*, pages 69–80. Springer, 2017.
- [37] C. Lehrenfeld and J. Schöberl. High order exactly divergence-free hybrid discontinuous Galerkin methods for unsteady incompressible flows. *Comput. Methods Appl. Mech. Engrg.*, 307:339–361, 2016.
- [38] Alexander Lindsay, Guillaume Giudicelli, Peter German, John Peterson, Yaqi Wang, Ramiro Freile, David Andrs, Paolo Balestra, Mauricio Tano, Rui Hu, et al. Moose navier–stokes module. *SoftwareX*, 23:101503, 2023.
- [39] Y. Liu, P. Ghysels, L. Claus, and X. S. Li. Sparse approximate multifrontal factorization with butterfly compression for high-frequency wave equations. *SIAM Journal on Scientific Computing*, 43(5):S367–S391, 2021.
- [40] P. Lu, A. Rupp, and G. Kanschat. Analysis of injection operators in geometric multigrid solvers for HDG methods. *SIAM J. Numer. Anal.*, 60(4):2293–2317, 2022.
- [41] T. A. Manteuffel, S. Münzenmaier, J. Ruge, and B. S. Southworth. Nonsymmetric reduction-based algebraic multigrid. *SIAM J. Sci. Comput.*, 41(5):S242–S268, 2019.
- [42] T. A. Manteuffel, J. W. Ruge, and B. S. Southworth. Nonsymmetric algebraic multigrid based on local approximate ideal restriction (ℓ AIR). *SIAM Journal on Scientific Computing*, 40(6):A4105–A4130, 2018.
- [43] Bijan Mohammadi and Olivier Pironneau. Analysis of the k-epsilon turbulence model. 1993.
- [44] S. Muralikrishnan, T. Bui-Thanh, and J. N. Shadid. A multilevel approach for trace system in HDG discretizations. *J. Comput. Phys.*, 407, 2020.
- [45] N. C. Nguyen, J. Peraire, and B. Cockburn. An implicit high-order hybridizable discontinuous Galerkin method for the incompressible Navier–Stokes equations. *J. Comput. Phys.*, 230(4):1147–1170, 2011.
- [46] Suhas Patankar. *Numerical heat transfer and fluid flow*. CRC press, 2018.
- [47] W. Qiu and K. Shi. A superconvergent HDG method for the incompressible Navier–Stokes equations on general polyhedral meshes. *IMA J. Numer. Anal.*, 36(4):1943–1967, 2016.
- [48] S. Rhebergen and G. Wells. A hybridizable discontinuous Galerkin method for the Navier–Stokes equations with pointwise divergence-free velocity field. *J. Sci. Comput.*, 76(3):1484–1501, 2018.
- [49] S. Rhebergen and G. N. Wells. Analysis of a hybridized/interface stabilized finite element method for the Stokes equations. *SIAM J. Numer. Anal.*, 55(4):1982–2003, 2017.
- [50] S. Rhebergen and G. N. Wells. Preconditioning of a hybridized discontinuous galerkin finite element method for the Stokes equations. *J. Sci. Comput.*, 77(3):1936–1952, 2018.
- [51] S. Rhebergen and G. N. Wells. An embedded-hybridized discontinuous Galerkin finite element method for the Stokes equations. *Comput. Methods Appl. Mech. Engrg.*, 358, 2020.
- [52] Pierre Sagaut. *Large eddy simulation for incompressible flows: an introduction*. Springer, 2006.

- [53] A. A. Sivas. *Preconditioning of hybridizable discontinuous Galerkin discretizations of the Navier–Stokes equations*. PhD thesis, University of Waterloo, 2021.
- [54] A. A. Sivas, B. S. Southworth, and S. Rhebergen. AIR algebraic multigrid for a space-time hybridizable discontinuous Galerkin discretization of advection(-diffusion). *SIAM Journal on Scientific Computing*, 43(5):A3393–A3416, 2021.
- [55] Joseph Smagorinsky. General circulation experiments with the primitive equations: I. the basic experiment. *Monthly weather review*, 91(3):99–164, 1963.
- [56] B. S. Southworth, A. A. Sivas, and S. Rhebergen. On fixed-point, Krylov, and 2x2 block preconditioners for nonsymmetric problems. *SIAM J. Matrix. Anal. A.*, 41(2):871–900, 2020.
- [57] Henk Kaarle Versteeg. *An introduction to computational fluid dynamics the finite volume method, 2/E*. Pearson Education India, 2007.

A Proof of Lemma 2

Consider the following two problems: Find $u_h^\gamma \in V_h$ such that

$$(u_h^\gamma, v_h)_\mathcal{T} + \gamma \langle h_F^{-1} \llbracket u_h^\gamma \cdot n \rrbracket, \llbracket v_h \cdot n \rrbracket \rangle_{\mathcal{F}} = (g, v_h)_\mathcal{T} \quad \forall v_h \in V_h, \quad (27)$$

and: Find $(u_h, \bar{p}_h) \in V_h \times \bar{Q}_h$ such that

$$(u_h, v_h)_\mathcal{T} + \langle \bar{p}_h, \llbracket v_h \cdot n \rrbracket \rangle_{\mathcal{F}} = (g, v_h)_\mathcal{T} \quad \forall v_h \in V_h, \quad (28a)$$

$$\langle \llbracket u_h \cdot n \rrbracket, \bar{q}_h \rangle_{\mathcal{F}} - \gamma^{-1} \langle h_F \bar{p}_h, \bar{q}_h \rangle_{\mathcal{F}} = 0 \quad \forall \bar{q}_h \in \bar{Q}_h. \quad (28b)$$

Step 1. We will start by proving that eq. (27) and eq. (28) are equivalent in the sense that if $(u_h, \bar{p}_h) \in V_h \times \bar{Q}_h$ solves eq. (28) and $u_h^\gamma \in V_h$ solves eq. (27), then $u_h = u_h^\gamma$ and $\bar{p}_h = \gamma h_F^{-1} \llbracket u_h^\gamma \cdot n \rrbracket$. Subtract eq. (28a) from eq. (27):

$$(u_h^\gamma - u_h, v_h)_\mathcal{T} + \gamma \langle h_F^{-1} \llbracket u_h^\gamma \cdot n \rrbracket, \llbracket v_h \cdot n \rrbracket \rangle_{\mathcal{F}} = \langle \bar{p}_h, \llbracket v_h \cdot n \rrbracket \rangle_{\mathcal{F}} \quad \forall v_h \in V_h.$$

Choose $v_h = u_h^\gamma - u_h$, then

$$\|u_h^\gamma - u_h\|_\Omega^2 + \gamma \langle h_F^{-1} \llbracket u_h^\gamma \cdot n \rrbracket, \llbracket u_h^\gamma \cdot n \rrbracket \rangle_{\mathcal{F}} - \gamma \langle h_F^{-1} \llbracket u_h^\gamma \cdot n \rrbracket, \llbracket u_h \cdot n \rrbracket \rangle_{\mathcal{F}} = \langle \bar{p}_h, \llbracket u_h^\gamma \cdot n \rrbracket \rangle_{\mathcal{F}} - \langle \bar{p}_h, \llbracket u_h \cdot n \rrbracket \rangle_{\mathcal{F}}. \quad (29)$$

By choosing $\bar{q}_h = h_F^{-1} \llbracket u_h^\gamma \cdot n \rrbracket$ and $\bar{q}_h = h_F^{-1} \llbracket u_h \cdot n \rrbracket$ in eq. (28b) we find, respectively,

$$\langle \bar{p}_h, \llbracket u_h^\gamma \cdot n \rrbracket \rangle_{\mathcal{F}} = \gamma \langle \llbracket u_h \cdot n \rrbracket, h_F^{-1} \llbracket u_h^\gamma \cdot n \rrbracket \rangle_{\mathcal{F}}, \quad \langle \bar{p}_h, \llbracket u_h \cdot n \rrbracket \rangle_{\mathcal{F}} = \gamma \langle \llbracket u_h \cdot n \rrbracket, h_F^{-1} \llbracket u_h \cdot n \rrbracket \rangle_{\mathcal{F}}.$$

Using these expressions in eq. (29),

$$\|u_h^\gamma - u_h\|_\Omega^2 + \gamma \langle h_F^{-1} \llbracket u_h^\gamma \cdot n \rrbracket, \llbracket u_h^\gamma \cdot n \rrbracket \rangle_{\mathcal{F}} - 2\gamma \langle h_F^{-1} \llbracket u_h^\gamma \cdot n \rrbracket, \llbracket u_h \cdot n \rrbracket \rangle_{\mathcal{F}} = -\gamma \langle h_F^{-1} \llbracket u_h \cdot n \rrbracket, \llbracket u_h \cdot n \rrbracket \rangle_{\mathcal{F}}.$$

We may write this as:

$$\|u_h^\gamma - u_h\|_\Omega^2 + \gamma \|h_F^{-1} \llbracket (u_h^\gamma - u_h) \cdot n \rrbracket\|_{\Gamma_0}^2 - \gamma \langle h_F^{-1} \llbracket u_h \cdot n \rrbracket, \llbracket u_h \cdot n \rrbracket \rangle_{\mathcal{F}} = -\gamma \langle h_F^{-1} \llbracket u_h \cdot n \rrbracket, \llbracket u_h \cdot n \rrbracket \rangle_{\mathcal{F}},$$

in other words, $\|u_h^\gamma - u_h\|_\Omega^2 + \gamma \|h_F^{-1} \llbracket (u_h^\gamma - u_h) \cdot n \rrbracket\|_{\Gamma_0}^2 = 0$ implying that $u_h = u_h^\gamma$. To now show that $\bar{p}_h = \gamma h_F^{-1} \llbracket u_h^\gamma \cdot n \rrbracket$, use $u_h = u_h^\gamma$ in eq. (28b) to find that $\langle \gamma \llbracket u_h^\gamma \cdot n \rrbracket - h_F \bar{p}_h, \bar{q}_h \rangle_{\mathcal{F}_h} = 0$ for all $\bar{q}_h \in \bar{Q}_h$. Choosing $\bar{q}_h = \gamma \llbracket u_h^\gamma \cdot n \rrbracket - h_F \bar{p}_h$ we obtain $\|\gamma \llbracket u_h^\gamma \cdot n \rrbracket - h_F \bar{p}_h\|_{\Gamma_0}^2 = 0$ implying that $\bar{p}_h = \gamma h_F^{-1} \llbracket u_h^\gamma \cdot n \rrbracket$.

Step 2. With the equivalence between eq. (27) and eq. (28) established, we write both problems in matrix form. Equation (27) in matrix form is given by:

$$(M_u + \gamma D_{uu})u = G, \quad (30)$$

where M_u is the mass matrix on the cell velocity space. Noting that $\langle \bar{q}_h, \llbracket v_h \cdot n \rrbracket \rangle_{\mathcal{F}} = \langle \bar{q}_h, v_h \cdot n \rangle_{\partial\mathcal{T}} = b_2(\bar{q}_h, v_h)$, eq. (28) in matrix form is given by:

$$\begin{bmatrix} M_u & B_{\bar{p}u}^T \\ B_{\bar{p}u} & -\gamma^{-1}\bar{M} \end{bmatrix} \begin{bmatrix} u \\ \bar{p} \end{bmatrix} = \begin{bmatrix} G \\ 0 \end{bmatrix}. \quad (31)$$

Eliminating \bar{p} from eq. (31), we obtain the following equation for u :

$$(M_u + \gamma B_{\bar{p}u}^T \bar{M}^{-1} B_{\bar{p}u})u = G. \quad (32)$$

The result follows by comparing eq. (30) and eq. (32).

B Well-posedness and a priori error analysis

Here we present a well-posedness and a priori error analysis of eq. (24). For the Navier–Stokes equations eq. (1) with homogeneous Dirichlet boundary conditions and constant viscosity μ we note that we can replace $-\nabla \cdot (2\mu\varepsilon(u))$ by $-\mu\nabla^2 u$. This simplification is used in this section to analyze eq. (24).

Well-posedness and an a priori error analysis of eq. (24) with $\gamma = 0$ was proven in [31]. Although $g_h(\cdot, \cdot)$ eq. (19) is a consistent penalty term, the nullspace of g_h is a subspace of $V_h \cap H(\text{div}; \Omega)$ and so the solution to eq. (24) will depend on γ . To determine the effect of γ , we generalize the results of [31] to $\gamma \geq 0$. We will require the following (semi-)norms on the extended velocity space $\mathbf{V}(h) := \mathbf{V}_h + (H_0^1(\Omega)^d \cap H^2(\Omega)^d) \times H_0^{3/2}(\Gamma^0)^d$:

$$\begin{aligned} \|\mathbf{v}\|_v^2 &:= \sum_{K \in \mathcal{T}_h} \left(\|\nabla v\|_K^2 + h_K^{-1} \|\bar{v} - v\|_{\partial K}^2 \right), & \|\mathbf{v}\|_{v'}^2 &:= \|\mathbf{v}\|_v^2 + \sum_{K \in \mathcal{T}_h} h_K \|\partial_n v\|_{\partial K}^2, \\ \|\mathbf{v}\|_{v,\gamma}^2 &:= \|\mathbf{v}\|_v^2 + \gamma \mu^{-1} |\mathbf{v}|_r^2, & \|\mathbf{v}\|_{v',\gamma}^2 &:= \|\mathbf{v}\|_{v'}^2 + \gamma \mu^{-1} |\mathbf{v}|_r^2. \end{aligned}$$

where $|\mathbf{v}|_r^2 := \sum_{K \in \mathcal{T}_h} h_K^{-1} \|(v - \bar{v}) \cdot n\|_{\partial K}^2$. For $v \in V(h) := V_h + H_0^1(\Omega)^d \cap H^2(\Omega)^d$ we set $\|v\|_{1,h} := \|\mathbf{v}\|_v$ and note that

$$\|\mathbf{v}\|_{v,\gamma} = \|\mathbf{v}\|_v \quad \forall v \in V(h) \cap H(\text{div}; \Omega). \quad (33)$$

Furthermore, by [9, Proposition A.2],

$$\|v\|_{\Omega} \leq c \|v\|_{1,h} \leq c \|\mathbf{v}\|_v \quad \forall v \in \mathbf{V}(h). \quad (34)$$

On the extended pressure space $\mathbf{Q}(h) := \mathbf{Q}_h + (L_0^2(\Omega) \cap H^1(\Omega)) \times H_0^{1/2}(\Gamma^0)$ we define the norm

$$\|\mathbf{q}\|_p^2 := \|q\|_{\Omega}^2 + \sum_{K \in \mathcal{T}_h} h_K \|\bar{q}\|_{\partial K}^2.$$

Finally, we define

$$\|\mathbf{v}_h, \mathbf{q}_h\|_{v,\gamma,p}^2 := \mu \|\mathbf{v}_h\|_{v,\gamma}^2 + \mu^{-1} \|\mathbf{q}_h\|_p^2 \quad \forall (\mathbf{v}_h, \mathbf{q}_h) \in \mathbf{V}_h \times \mathbf{Q}_h.$$

Note that

$$\begin{aligned} a_h(\mathbf{v}_h, \mathbf{v}_h) &\geq c \|\mathbf{v}_h\|_v^2 & \forall \mathbf{v}_h \in \mathbf{V}_h, & \quad a_h(\mathbf{u}, \mathbf{v}) \leq c \|\mathbf{u}\|_{v'} \|\mathbf{v}\|_{v'}, & \quad \forall \mathbf{u}, \mathbf{v} \in \mathbf{V}(h), \\ g_h(\mathbf{v}_h, \mathbf{v}_h) &= |\mathbf{v}_h|_r^2 \geq 0 & \forall \mathbf{v}_h \in \mathbf{V}_h, & \quad |g_h(\mathbf{u}, \mathbf{v})| \leq |\mathbf{u}|_r |\mathbf{v}|_r & \quad \forall \mathbf{u}, \mathbf{v} \in \mathbf{V}(h), \end{aligned}$$

where the inequalities in the first row are shown in [49, Lemmas 4.2 and 4.3]. Combining these inequalities, and using Hölder's inequality, we note that

$$\begin{aligned} \mu a_h(\mathbf{u}, \mathbf{v}) + \gamma g_h(\mathbf{u}, \mathbf{v}) &\leq c \mu \|\mathbf{u}\|_{v',\gamma} \|\mathbf{v}\|_{v',\gamma} & \forall \mathbf{u}, \mathbf{v} \in \mathbf{V}(h), \\ \mu a_h(\mathbf{v}_h, \mathbf{v}_h) + \gamma g_h(\mathbf{v}_h, \mathbf{v}_h) &\geq c \mu \|\mathbf{v}_h\|_{v,\gamma}^2 & \forall \mathbf{v}_h \in \mathbf{V}_h. \end{aligned}$$

By [9, Proposition 3.6] we have for $w_h \in \{v_h \in V_h : b_h(\mathbf{q}_h, v_h) = 0 \ \forall \mathbf{q}_h \in \mathbf{Q}_h\}$,

$$o_h(w_h; \mathbf{v}_h, \mathbf{v}_h) \geq 0 \quad \forall \mathbf{v}_h \in \mathbf{V}_h,$$

and by [9, Proposition 3.4], for $w_1, w_2 \in V(h)$, $\mathbf{u} \in \mathbf{V}(h)$, and $\mathbf{v} \in \mathbf{V}(h)$, we have

$$|o_h(w_1; \mathbf{u}, \mathbf{v}) - o_h(w_2; \mathbf{u}, \mathbf{v})| \leq c \|w_1 - w_2\|_{1,h} \|\mathbf{u}\|_v \|\mathbf{v}\|_v.$$

For b_h we have that for all $\mathbf{v} \in \mathbf{V}(h)$ and $\mathbf{q} \in \mathbf{Q}(h)$ [49, Lemma 4.8]:

$$|b_h(\mathbf{q}, v)| \leq c \|\mathbf{v}\|_v \|\mathbf{q}\|_p \leq c \|\mathbf{v}\|_{v,\gamma} \|\mathbf{q}\|_p.$$

An inf-sup condition for b_h in terms of $\|\cdot\|_v$ was proven in [50, Lemma 1]. The following lemma proves an inf-sup condition with respect to $\|\cdot\|_{v,\gamma}$.

Lemma 3 (inf-sup condition). *There exists a constant $c > 0$, independent of h, μ, γ , such that*

$$\sup_{\mathbf{0} \neq \mathbf{v}_h \in \mathbf{V}_h} \frac{b_h(\mathbf{q}_h, v_h)}{\|\mathbf{v}_h\|_{v,\gamma}} \geq c \|\mathbf{q}_h\|_p \quad \forall \mathbf{q}_h \in \mathbf{Q}_h.$$

Proof. **Step 1.** Define the following two spaces:

$$\begin{aligned} \mathbf{Ker}(g_h) &:= \{\mathbf{v}_h \in \mathbf{V}_h : ((v_h - \bar{v}_h) \cdot \mathbf{n})|_F = 0 \ \forall F \in \mathcal{F}_h\}, \\ \mathbf{Ker}(b_2) &:= \{\mathbf{v}_h \in \mathbf{V}_h : v_h \in H(\text{div}; \Omega)\}, \end{aligned}$$

Let $\Pi_V : H^1(\Omega)^d \rightarrow V_h$ be the BDM interpolation operator [8, Section III.3]. Note that for all $v \in H^1(\Omega)^d$ we have that $(\Pi_V v, \{\{\Pi_V v\}\}) \in \mathbf{Ker}(g_h)$ and, using eq. (33),

$$\|(\Pi_V v, \{\{\Pi_V v\}\})\|_{v,\gamma} \leq c \|\Pi_V v\|_{1,h} \leq c \|v\|_{1,\Omega}, \quad (35)$$

where the second inequality was shown in [26, Proposition 10]. For a $q_h \in \mathbf{Q}_h$ there exists a $v_{q_h} \in H_0^1(\Omega)^d$ such that $\nabla \cdot v_{q_h} = q_h$ and $c \|v_{q_h}\|_{1,\Omega} \leq \|q_h\|_\Omega$ (see, for example, [17, Theorem 6.5]). Using eq. (35), $\|(\Pi_V v_{q_h}, \{\{\Pi_V v_{q_h}\}\})\|_{v,\gamma} \leq c \|q_h\|_\Omega$. We find:

$$\sup_{\mathbf{0} \neq \mathbf{v}_h \in \mathbf{Ker}(b_2)} \frac{b_h((q_h, 0), v_h)}{\|\mathbf{v}_h\|_{v,\gamma}} \geq \sup_{\mathbf{0} \neq \mathbf{v}_h \in \mathbf{Ker}(g_h)} \frac{b_h((q_h, 0), v_h)}{\|\mathbf{v}_h\|_{v,\gamma}} \geq \frac{b_h((q_h, 0), \Pi_V v_{q_h})}{\|(\Pi_V v_{q_h}, \{\{\Pi_V v_{q_h}\}\})\|_{v,\gamma}} \geq c \|q_h\|_\Omega, \quad (36)$$

where the first inequality is because $\mathbf{Ker}(g_h) \subset \mathbf{Ker}(b_2)$.

Step 2. Let $L^{BDM} : R_k(\partial K) \rightarrow P_k(K)^d$ be the BDM local lifting operator such that $(L^{BDM} \mu) \cdot \mathbf{n} = \mu$ and $\|L^{BDM} \mu\|_K \leq ch_K^{1/2} \|\mu\|_{\partial K}$ for all $\mu \in R_k(\partial K)$ (see [19, Proposition 2.10]). Then, using eq. (33), eq. (34), and [50, Eq. (25)],

$$\|(L^{BDM} \bar{q}_h, \{\{L^{BDM} \bar{q}_h\}\})\|_{v,\gamma} \leq c \|L^{BDM} \bar{q}_h\|_{1,h} \leq c \|(L^{BDM} \bar{q}_h, 0)\|_v \leq c \sum_{K \in \mathcal{T}_h} h_K^{-1/2} \|\bar{q}_h\|_{\partial K}.$$

Identical steps as in [50, Lemma 3] then results in

$$\sup_{\mathbf{0} \neq \mathbf{v}_h \in \mathbf{V}_h} \frac{b_h((0, \bar{q}_h), v_h)}{\|\mathbf{v}_h\|_{v,\gamma}} \geq c \|(0, \bar{q}_h)\|_p. \quad (37)$$

Step 3. Since $\mathbf{Ker}(b_2) = \{\mathbf{v}_h \in \mathbf{V}_h : b_h((0, \bar{q}_h), \mathbf{v}_h) = 0 \ \forall \bar{q}_h \in \mathbf{Q}_h\}$, the result follows after combining eq. (36), eq. (37), and [29, Theorem 3.1]. \square

The next lemma proves well-posedness of eq. (24) by using the aforementioned properties of the forms a_h, g_h, o_h , and b_h .

Lemma 4 (Well-posedness). *The HDG discretization eq. (24) of the Navier–Stokes equations is well-posed for $\gamma \geq 0$. Furthermore, the solution $(\mathbf{u}_h, \mathbf{p}_h) \in \mathbf{V}_h \times \mathbf{Q}_h$ to eq. (24) satisfies:*

$$\|\mathbf{u}_h\|_{v,\gamma} \leq c\mu^{-1} \|f\|_{\Omega}, \quad \|(\mathbf{u}_h, \mathbf{p}_h)\|_{v,\gamma,p} \leq c \|f\|_{\Omega} + c\nu^{-2} \|f\|_{\Omega}^2.$$

Proof. The proof is identical to that of [31, Lemma 1] but with $a_h(\cdot, \cdot)$ replaced by $a_h(\cdot, \cdot) + \gamma g_h(\cdot, \cdot)$ and $\|\cdot\|_v$ replaced by $\|\cdot\|_{v,\gamma}$. \square

Let $\Pi_V : H^1(\Omega)^d \rightarrow V_h$ again be the BDM interpolation operator. Furthermore, let $\bar{\Pi}_V u$ be defined such that when restricted to a face F then $\bar{\Pi}_V u|_F = \{\{\Pi_V u\}\}$. Define $e_u^I = u - \Pi_V u$, $\bar{e}_u^I = \bar{u} - \bar{\Pi}_V u$, and $\mathbf{e}_u^I = (e_u^I, \bar{e}_u^I)$, where $\bar{u} = u|_{\Gamma^0}$. Furthermore, let $\bar{\Pi}_{L^2(\Gamma^0)}$ be the standard L^2 -projection operator onto \bar{V}_h .

The following lemma now determines error estimates for the discrete velocity and pressure. We will write $h := \max_{K \in \mathcal{T}_h} h_K$.

Lemma 5 (Error estimates). *Let $(u, p) \in H^{k+1}(\Omega)^d \times H^k(\Omega)$ be the solution to the Navier–Stokes equations eq. (1), $\mathbf{u} = (u, \bar{u})$, $\mathbf{p} = (p, \bar{p})$, and $(\mathbf{u}_h, \mathbf{p}_h) \in \mathbf{V}_h \times \mathbf{Q}_h$ the solution to eq. (24) and assume that $\|f\|_{\Omega} \leq c\mu^2$. Then*

$$\|\mathbf{u} - \mathbf{u}_h\|_{v,\gamma} \leq ch^k \|u\|_{k+1,\Omega}, \quad \|p - p_h\|_{\Omega} \leq ch^k \|p\|_k + c\mu h^k \|u\|_{k+1,\Omega}.$$

Proof. Consider first the velocity error estimate. We have

$$\|\mathbf{u} - \mathbf{u}_h\|_{v,\gamma} \leq c \|\mathbf{e}_u^I\|_{v',\gamma} = c \|\mathbf{e}_u^I\|_{v'} = c \left(\|e_u^I\|_{1,h}^2 + \sum_{K \in \mathcal{T}_h} \|\partial_n e_u^I\|_{\partial K}^2 \right)^{1/2} \leq c \|\mathbf{e}_u^I, u - \bar{\Pi}_{L^2(\Gamma^0)} u\|_{v'}, \quad (38)$$

where the first inequality can be shown using identical steps as in the proof of [31, Theorem 1], but with $a_h(\cdot, \cdot)$ replaced by $a_h(\cdot, \cdot) + \gamma g_h(\cdot, \cdot)$, $\|\cdot\|_v$ replaced by $\|\cdot\|_{v,\gamma}$, and $\|\cdot\|_{v'}$ replaced by $\|\cdot\|_{v',\gamma}$. The first equality is by eq. (33), the second equality is by definition of $\|\cdot\|_{1,h}$, and the last inequality is by eq. (34). The result follows by using [51, Lemma 9].

For the pressure error estimate, replace $a_h(\cdot, \cdot)$ by $a_h(\cdot, \cdot) + \gamma g_h(\cdot, \cdot)$, $\|\cdot\|_v$ by $\|\cdot\|_{v,\gamma}$, and $\|\cdot\|_{v'}$ by $\|\cdot\|_{v',\gamma}$ in the proof of [31, Lemma 3] to find

$$\|p - p_h\|_{\Omega} \leq ch^k \|p\|_k + c\mu \|\mathbf{e}_u^I\|_{v',\gamma}.$$

The result follows after using the same steps as used in eq. (38) to bound $\|\mathbf{e}_u^I\|_{v',\gamma}$. \square

C More on Schur complement preconditioners and their PETSc implementation

As described in [2] the inverse of the Schur complement factorization is implemented in PETSc as

$$\begin{pmatrix} A_{00}^{-1} & 0 \\ 0 & I \end{pmatrix} \begin{pmatrix} I & -A_{01} \\ 0 & I \end{pmatrix} \begin{pmatrix} I & 0 \\ 0 & S^{-1} \end{pmatrix} \begin{pmatrix} I & 0 \\ -A_{10}A_{00}^{-1} & I \end{pmatrix} \quad (39)$$

Inverses are approximated via Krylov subspace solvers—denoted KSP in PETSc. PETSc offers various levels of completeness of eq. (39). One is `full` which includes all the components of eq. (39). The `lower` factorization option, which is what is used in all field splits outlined in this paper, drops a block matrix multiplication, and after some rearrangement yields:

$$\begin{pmatrix} I & 0 \\ 0 & S^{-1} \end{pmatrix} \begin{pmatrix} I & 0 \\ -A_{10} & I \end{pmatrix} \begin{pmatrix} A_{00}^{-1} & 0 \\ 0 & I \end{pmatrix} \quad (40)$$

Equation (40) explicitly requires only one A_{00}^{-1} approximate inversion via KSP, which is known as the `lower` KSP after our lower factorization choice. However, we note that approximate inversion of S via a Krylov subspace solver involves multiplication by S which itself introduces additional KSP(A_{00}) because $S = A_{11} - A_{10} \text{KSP}(A_{00}) A_{01}$. Consequently every iteration of KSP(S) involves a nested/inner solve of KSP(A_{00}). PETSc allows specifying different preconditioning options for lower and inner KSP(A_{00}) solves, but by default it uses the same preconditioning options for both cases.